Home   Search   Collections   Journals   About   Contact us   My IOPscience

Production and decay of the ^{73}Ge*(1/2$^-$) metastable state in a low-background germanium detector

View the table of contents for this issue, or go to the journal homepage for more

RESEARCH NOTE FROM COLLABORATION

Production and decay of the ^{73}Ge*$(1/2^-)$ metastable state in a low-background germanium detector

H Y Liao[1,2], **H M Chang**[1,2], **M H Chou**[1], **M Deniz**[1,3], **H X Huang**[1,4],
F S Lee[1], **H B Li**[1], **J Li**[5,6], **C W Lin**[1], **F K Lin**[1], **S K Lin**[1], **S T Lin**[1],
V Singh[1], **H T Wong**[1] **and S C Wu**[1] **(TEXONO Collaboration)**

[1] Institute of Physics, Academia Sinica, Taipei 115, Taiwan
[2] Department of Physics, National Taiwan University, Taipei 106, Taiwan
[3] Department of Physics, Middle East Technical University, Ankara 06531, Turkey
[4] Department of Nuclear Physics, Institute of Atomic Energy, Beijing 102413,
People's Republic of China
[5] Institute of High Energy Physics, Chinese Academy of Science, Beijing 100039,
People's Republic of China
[6] Department of Engineering Physics, Tsing Hua University, Beijing 100084,
People's Republic of China

E-mail: htwong@phys.sinica.edu.tw

Abstract
The ^{73}Ge*$(1/2^-)$ metastable state decays with a very characteristic signature which allows it to be tagged event-by-event. Studies were performed using data taken with a high-purity germanium detector in a low-background laboratory near a nuclear power reactor core where the $\bar{\nu}_e$-flux was 6.4×10^{12} cm^{-2} s^{-1}. The measured average and equilibrium production rates of ^{73}Ge*$(1/2^-)$ were (8.7 ± 0.4) and (6.7 ± 0.3) kg^{-1} day^{-1}, respectively. The production channels were studied and identified. By studying the difference in the production of ^{73}Ge*$(1/2^-)$ between the reactor ON and OFF spectra, limiting sensitivities in the range of $\sim 10^{-42}$ to 10^{-43} cm^2 for the cross sections of neutrino-induced nuclear transitions were derived. The dominant backgrounds are due to β^- decays of cosmic-ray-induced ^{73}Ga. The prospects of enhancing the sensitivities at underground locations are discussed.

(Some figures in this article are in colour only in the electronic version)

1. Introduction

A research program on low-energy neutrino physics [1] is being pursued by the TEXONO Collaboration at the Kuo-Sheng (KS) Reactor Laboratory in Taiwan [2]. A search for the neutrino magnetic moment [3] was performed with an ultra-low-background high-purity
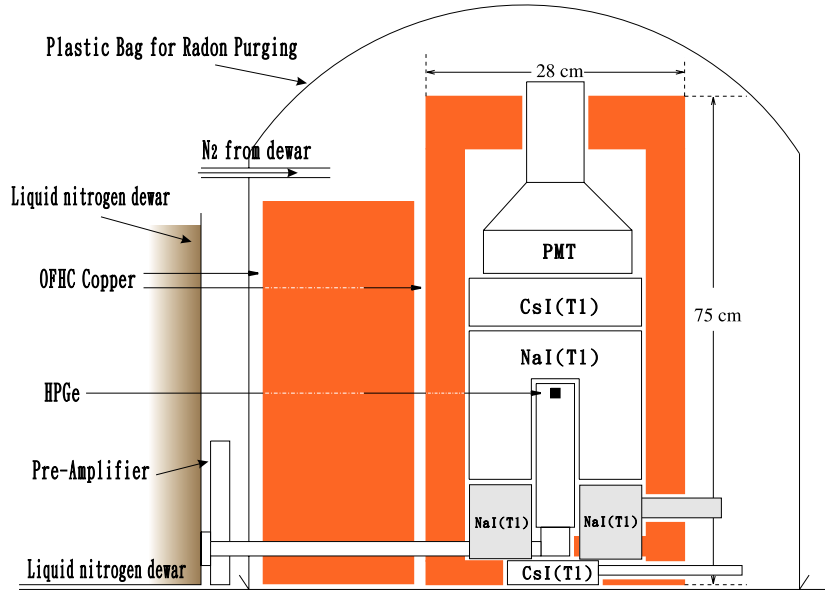
Figure 1. Schematic layout of the HPGe with its anti-Compton detectors as well as inner shieldings and radon purge system.

germanium detector (HPGe), from which a limit of $\mu_\nu(\bar{\nu}_e) < 7.4 \times 10^{-11} \mu_B$ at 90% confidence level (CL) was derived [8]. During the course of this study, the unique signature of the decay of the ^{73}Ge*$(1/2^-)$ metastable state was noted.

In this note, we discuss these decay signatures in section 2 and present studies of their production channels in section 3. These investigations are of relevance to the understanding of backgrounds in this and other germanium-based low-background experiments, such as those on double-beta decays [4, 5] and cold dark-matter searches [6, 7]. Moreover, the data also allow the evaluations of the experimental sensitivities of various neutrino-induced nuclear transitions in reactor neutrino experiments under realistic conditions, the studies of which are discussed in section 4.

2. Experimental signatures of ^{73}Ge*$(1/2^-)$ decays

The experimental details, including detector hardware, shieldings, electronics systems as well as studies of systematic uncertainties, are discussed in [8]. The schematics of the experimental set-up is shown in figure 1. The laboratory is located at a distance of 28 m from a nuclear reactor core with a thermal power output of 2.9 GW. The total reactor-$\bar{\nu}_e$ flux is about 6.4×10^{12} cm^{-2} s^{-1}. The $\bar{\nu}_e$ spectrum is shown in figure 2. The $\bar{\nu}_e$'s are emitted via β^- decays of (a) fission fragments and (b) ^{239}U following neutron capture on ^{238}U.

The natural isotopic abundance of ^{73}Ge in germanium is 7.73%. The level schemes for the isobaric states of ^{73}Ga, ^{73}Ge and ^{73}As relevant to this note are depicted in figure 3 [11]. The ^{73}Ge*$(1/2^-)$ metastable nuclei decay via the emissions of 53.4 keV and 13.3 keV photons separated by a half-life of 2.9 μs. This characteristic delayed coincidence gives an experimental signature which can be uniquely identified in a HPGe detector.

The HPGe target was 1.06 kg in mass and was surrounded by active anti-Compton veto (ACV) detectors made of NaI(Tl) and CsI(Tl) scintillating crystals. The detector system was
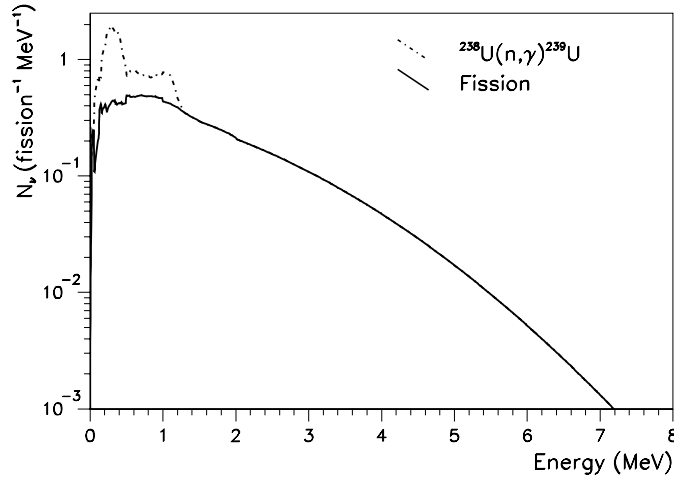
Figure 2. Total $\bar{\nu}_e$-spectra at the power reactor, showing the two components due to β^- decays of fission fragments and ^{239}U.
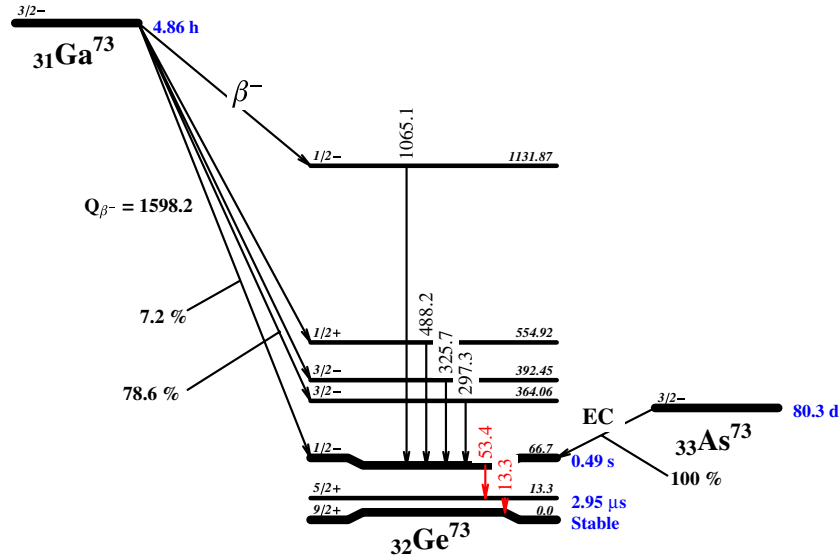

Figure 3. The ^{73}Ge production and decay scheme [11] relevant to the discussions in this note.

placed inside a 50-ton shielding structure with an outermost layer of plastic scintillator panels acting as cosmic-ray veto (CRV). A physics threshold of 12 keV and a background level of ~ 1 kg^{-1} keV^{-1} day^{-1} comparable to those of underground dark matter experiments were achieved. Besides magnetic moment searches, this unique data set also allows the studies of ν_e [9] and the searches for axions [10] from the power reactor.

Events uncorrelated with the CRV and ACV are candidates for neutrino-induced signals. The performance and efficiencies of these selections were thoroughly studied and documented in [8]. The amplitude-versus-energy plot for the 'after-cut' events is displayed in figure 4. The conspicuous structure at 66.7 keV is due to the convoluted sum of two correlated events
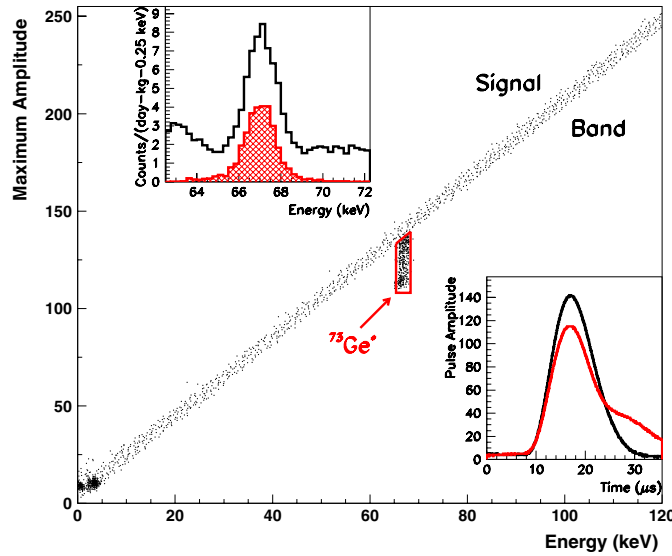
Figure 4. Scatter plot of maximum amplitude versus energy for selected events, showing that decays from ^{73}Ge*$(1/2^-)$ nuclei can be identified perfectly. The energy spectra before (black) and after (red) event selection are shown in the left inset. Typical pulse shapes for normal (black) and ^{73}Ge*$(1/2^-)$ (red) events are displayed in the right inset.

delayed relative to one another, identified unambiguously as ^{73}Ge*$(1/2^-)$ decays. A typical event pair is shown in the inset of figure 4. This pulse-shape signature is very distinct and can be tagged at an event-by-event basis without contamination of background events.

Once the decays of ^{73}Ge*$(1/2^-)$ were tagged, their production channels can be studied. The data-acquisition (DAQ) system [12] records timing information for all events. This capability allows the decay sequences with half-lives as long as 55 s to be distinctly identified [13]. The KS-P1 (180.1/52.7 days reactor ON/OFF live time) and KS-P3 (278.9/43.6 days reactor ON/OFF live time) periods, as defined in [8], were used in the analysis. The total live times are 459.0/96.3 days for reactor ON/OFF, respectively. The selection efficiency of the ^{73}Ge*$(1/2^-)$ events is 85%, the missing fraction being those with the two γ's emitted closer than 0.16 s in time to each other. Data taken 5 s before and after these events were retrieved for subsequent detailed studies. The production of the ^{73}Ge*$(1/2^-)$ states takes place mostly in the interval of about 2 s (or 4 half-lives) *before* the ^{73}Ge*$(1/2^-)$ decays, while events from the other intervals represent the background control samples. After efficiency corrections, the production rates of the ^{73}Ge*$(1/2^-)$ nuclei were measured. The rates decreased within a DAQ period and are characterized by two quantities. The *average rates* represent the sum of all ^{73}Ge*$(1/2^-)$ decays divided by the total DAQ live time, while the *equilibrium rates* are the steady-state rates reached at the end of the DAQ periods. The average and equilibrium rates were (8.7 ± 0.4) kg^{-1} day^{-1} and (6.7 ± 0.3) kg^{-1} day^{-1}, respectively.
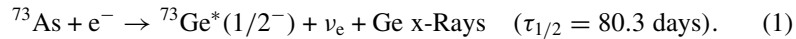
3. Production channels of ^{73}Ge*$(1/2^-)$

The identified production channels for ^{73}Ge*$(1/2^-)$ nuclei and their relative fractions are summarized in table 1. Specific signatures of individual channels are described in the following paragraphs. For simplicity, the 'BEFORE' and 'AFTER' spectra taken within the time interval

Table 1. Summary of the ^{73}Ge*$(1/2^-)$ production rates, and those of individual channels in the two data-taking periods.

DAQ periods	Measured event rate (day^{-1} kg^{-1})			Distribution (%)		
	P1	P3	Combined	P1	P3	Combined
^{73}Ge*$(1/2^-)$ production rate						
DAQ end (equilibrium)	8.8 ± 0.5	5.2 ± 0.4	6.7 ± 0.3	–	–	–
Average	9.9 ± 0.6	8.1 ± 0.5	8.7 ± 0.4	100.0	100.0	100.0
Production channels						
1. ^{73}As decays						
DAQ start	1.8 ± 0.2	1.8 ± 0.2	1.8 ± 0.2	–	–	–
DAQ end (equilibrium)	0.3 ± 0.1	0.2 ± 0.1	0.2 ± 0.1	–	–	–
Average	1.0 ± 0.1	0.7 ± 0.1	0.8 ± 0.1	9.8 ± 0.9	9.2 ± 0.8	9.5 ± 0.6
2. ^{73}Ga decays						
β^-	2.2 ± 0.2	1.9 ± 0.2	2.0 ± 0.1	21.7 ± 1.6	23.2 ± 1.6	22.5 ± 1.1
$\beta^- \gamma$ (full E_γ)	0.9 ± 0.1	0.7 ± 0.1	0.8 ± 0.1	9.1 ± 1.0	9.1 ± 0.9	9.1 ± 0.6
$\beta^- \gamma$ (partial E_γ)	1.0 ± 0.2	0.5 ± 0.1	0.6 ± 0.1	9.7 ± 1.4	5.6 ± 1.0	7.0 ± 0.8
3. Prompt cosmic-induced ^{73}Ge*$(1/2^-)$						
With CRV tag	2.2 ± 0.3	1.9 ± 0.3	2.0 ± 0.2	22.0 ± 2.8	23.9 ± 2.7	23.0 ± 2.0
HPGe only (no CRV)	0.0 ± 0.0	0.0 ± 0.0	0.0 ± 0.0	0.0 ± 0.1	0.3 ± 0.1	0.1 ± 0.1
HPGe+NaI (no CRV)	0.1 ± 0.1	0.1 ± 0.0	0.1 ± 0.0	1.1 ± 0.7	1.4 ± 0.5	1.3 ± 0.4
Total identified production channels for ^{73}Ge*$(1/2^-)$						
	7.3 ± 0.4	5.9 ± 0.3	6.4 ± 0.3	73.4 ± 3.8	72.7 ± 3.5	73.0 ± 2.6
Identified inefficiency factors						
DAQ dead time	–	–	–	4.3	8.5	6.6
Selection inefficiencies						
CRV+ACV cuts	–	–	–	5.0	8.0	6.6
$5\ \mathrm{ms} < \Delta t \leqslant 2\ \mathrm{s}$	–	–	–	7.1	7.1	7.1
Total identified percentage						
	–	–	–	89.8 ± 3.8	96.3 ± 3.5	93.3 ± 2.6

$(-2, 0)$ s and $(0, 2)$ s by the detector X (X can be NaI or Ge) are denoted by Φ_X^- and Φ_X^+, respectively.

(i) ^{73}*As*: The most conspicuous difference between the Φ_{Ge}^- and Φ_{Ge}^+ spectra, after the CRV and ACV cuts were applied, is the Ge x-ray peak at 11.1 keV depicted in figure 5. In contrast, the structure for Φ_{Ge}^+ peaks at 10.4 keV, corresponding to the Ga x-rays following the decays of ^{68}Ge which were uncorrelated with the ^{73}Ge*$(1/2^-)$ production. The timing distribution of the Φ_{Ge}^- events associated with the peak is shown in the inset. The best-fit half-life is (0.81 ± 0.22) s, in good agreement with expectation and demonstrating that the ^{73}Ge*$(1/2^-)$ states were really produced. The time variation of the event rates is depicted in figure 6(a). The best-fit half-life for the P3 data is (62.0 ± 23.8) days, consistent with the interpretations of the electron capture of ^{73}As:

$$^{73}\mathrm{As} + \mathrm{e}^- \rightarrow {}^{73}\mathrm{Ge}^*(1/2^-) + \nu_\mathrm{e} + \mathrm{Ge\ x\text{-}Rays} \quad (\tau_{1/2} = 80.3\ \mathrm{days}). \quad (1)$$

This decay profile indicates that the production of ^{73}As was cosmic-ray induced. The production rate was reduced by a factor of ~ 9 inside the 50-ton shielding structure at the KS laboratory where the overburden is about 30 meter-water-equivalent (mwe).
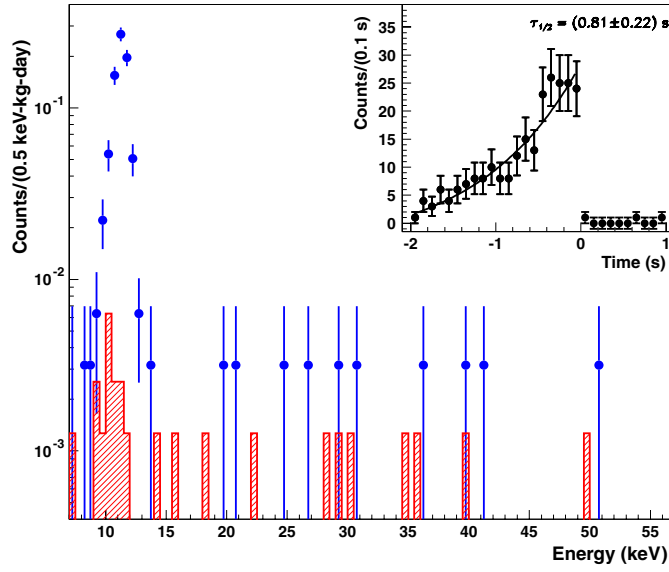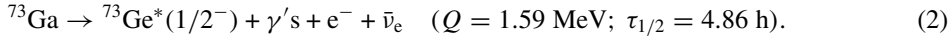
Figure 5. (a) Measured HPGe Φ_{Ge}^{-} (blue data points) and Φ_{Ge}^{+} (red histogram) spectra after ACV+CRV cuts from the P3 data. The time distribution of the Ge x-ray events in Φ_{Ge}^{-} is shown in the inset, verifying that ^{73}Ge*$(1/2^{-})$ nuclei were produced.

The steady-state equilibrium rate of (0.2 ± 0.1) kg^{-1} day^{-1} was reached after 400 days of data taking.

(ii) ^{73}Ga: The Φ_{Ge}^{-} and Φ_{Ge}^{+} spectra at the 1 MeV region for P3 are depicted in figures 7(a)–(c): (a) after CRV+ACV cuts, (b) after CRV cut, with signals at ACV corresponding to $E_{\gamma} \sim 300$ keV and (c) after CRV cut, with signals at ACV corresponding to $E_{\gamma} \neq 300$ keV. The timing distribution of the events is displayed in the inset of figures 7(a)–(c), verifying that ^{73}Ge*$(1/2^{-})$ nuclei were produced. These events are consistent with β^{-}-emissions from ^{73}Ga in the HPGe:

$$^{73}\text{Ga} \rightarrow {}^{73}\text{Ge*}(1/2^{-}) + \gamma\text{'s} + e^{-} + \bar{\nu}_{e} \quad (Q = 1.59 \text{ MeV}; \tau_{1/2} = 4.86 \text{ h}). \tag{2}$$

Some of the events in figure 7(a) are due to β^{-} decays which directly fed the ^{73}Ge*$(1/2^{-})$ state at a branching ratio (BR) of 7%. In addition, the β^{-} decays can also populate the various excited states, the dominant level of which is the $\frac{3}{2}^{-}$ state at BR = 78%, followed by γ-ray emissions at $E_{\gamma} = 297$ keV. The subsequent γ's were fully absorbed by the HPGe in about 57% of the decays, as indicated in table 1. These events also contribute to figure 7(a). The HPGe spectra where the $E_{\gamma} = 297$ keV photons were fully and partially absorbed by the NaI(Tl) AC detector are depicted in figures 7(b) and (c), respectively. The Φ_{NaI}^{-} and Φ_{NaI}^{+} spectra corresponding to the samples of figure 7(b) are displayed in figure 8, showing the detection of the line at $E_{\gamma} = 297$ keV.

(iii) *Prompt cosmic-induced* ^{73}Ge*$(1/2^{-})$: About 23% of the production of ^{73}Ge*$(1/2^{-})$ nuclei were in coincidence with a CRV tag. These events are usually characterized by large energy depositions and saturate the electronics in the HPGe or ACV detectors, as depicted in figure 9(a). For instance, one of the channels is the neutron capture on ^{72}Ge:

$$\text{n} + {}^{72}\text{Ge} \rightarrow {}^{73}\text{Ge*}(1/2^{-}) + \gamma\text{'s}, \tag{3}$$

where photons with total energy of as much as 8 MeV are generated. Only (15.8 ± 4.0)% of the events were of low energy where the electronics remained unsaturated (see also
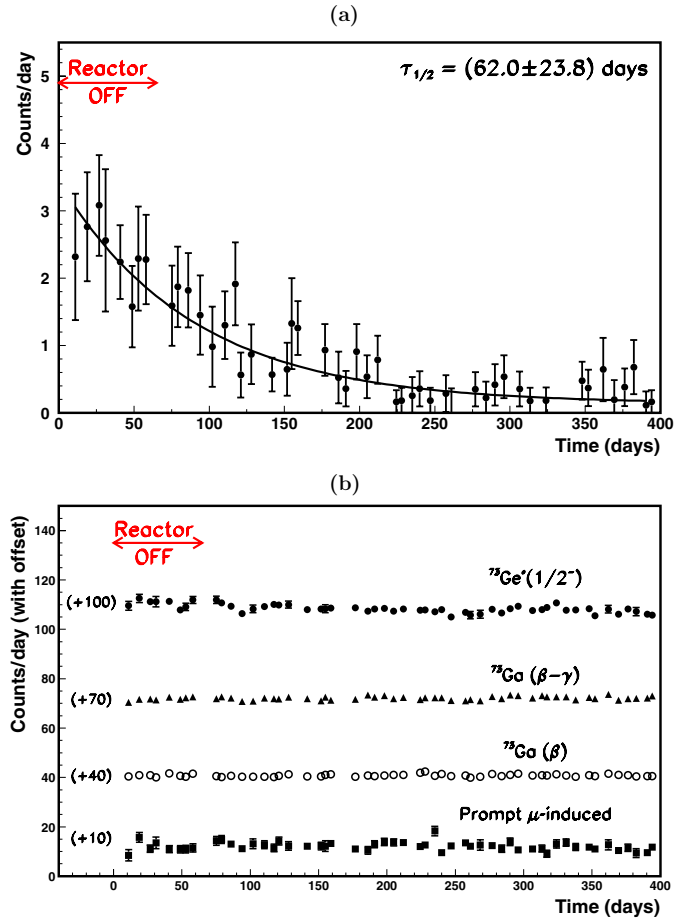
Figure 6. Time plot for the P3 data taking for event rates from (a) Ge x-rays, showing that they are due to the electron capture of ^{73}As to ^{73}Ge*$(1/2^-)$ and (b) other channels whose rates are stable. Offsets are introduced in (b) for visualization purposes. The data under ^{73}Ge*$(1/2^-)$ denote the steady-state production rate of ^{73}Ge*$(1/2^-)$ after the ^{73}As decays are taken into account.

figures 9(a) and (b)). There was an excess of events at about 300 keV for Φ^-_{NaI} over Φ^+_{NaI} due to γ-ray emissions from the $\frac{3}{2}^-$ (364 keV) excited state of ^{73}Ge. The corresponding energy depositions in the HPGe were less than 1 MeV. These events represent an evidence of the excitation of ^{73}Ge* through the interactions of high-energy neutrons produced by cosmic-ray-induced spallations in the ambient materials.

Among the tagged ^{73}Ge*$(1/2^-)$ events, 1.4% and (23% $\times$ 0.84) $\sim$ 19.3% are, respectively, those without and with CRV tags where the total energy depositions in the HPGe and AC detectors exceed the end point of ^{73}Ga β^- decays. This is consistent with an independent measurement of the CRV inefficiency of about 7% [8], due to geometrical coverage and hardware inefficiency. Accordingly, it can be concluded that all ^{73}Ge*$(1/2^-)$ nuclei produced with energy depositions above 1.6 MeV are associated with prompt cosmic rays.

After corrections on DAQ dead time and selection efficiencies, the identified production channel is about 93% of the tagged ^{73}Ge*$(1/2^-)$ decays. The missing events can be attributed
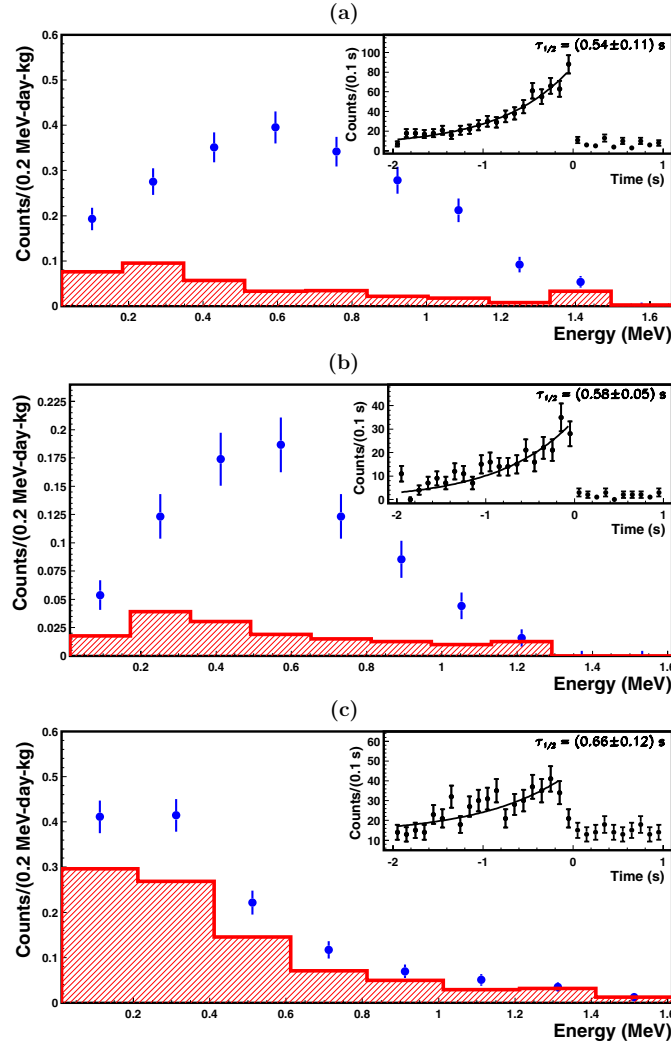
Figure 7. Measured Φ_{Ge}^{+} (red histogram) and Φ_{Ge}^{-} (blue data points) spectra in the 1 MeV region: (a) after CRV+ACV cuts, (b) after CRV cut, with signals at ACV corresponding to $E_{\gamma} \sim 300$ keV and (c) after CRV cut, with signals at ACV corresponding to $E_{\gamma} \neq 300$ keV. The inset shows the timing distribution of the Φ_{Ge}^{-} events.

to those which do not satisfy the DAQ trigger condition of having more than 5 keV energy deposition in the HPGe. An example of such channels is the production of ^{73}Ge*$(1/2^{-})$ or other ^{73}Ge* excited states via the excitation of high-energy neutrons, followed by complete escape of the final-state γ's from the HPGe.

All of the identified background is cosmic-ray induced, even though the decay time scales are vastly different: order of 100 days for ^{73}As, order of 10 h for ^{73}Ga and prompt signatures for those with a CRV tag. As illustrated in figures 6(a) and (b), the background rates of ^{73}As show the characteristic 80.3 day decay half-life, while the rates for the other background channels are constant with time. Accordingly, this background is expected to be greatly suppressed in an underground laboratory where the cosmic-ray fluxes are attenuated. The residual background
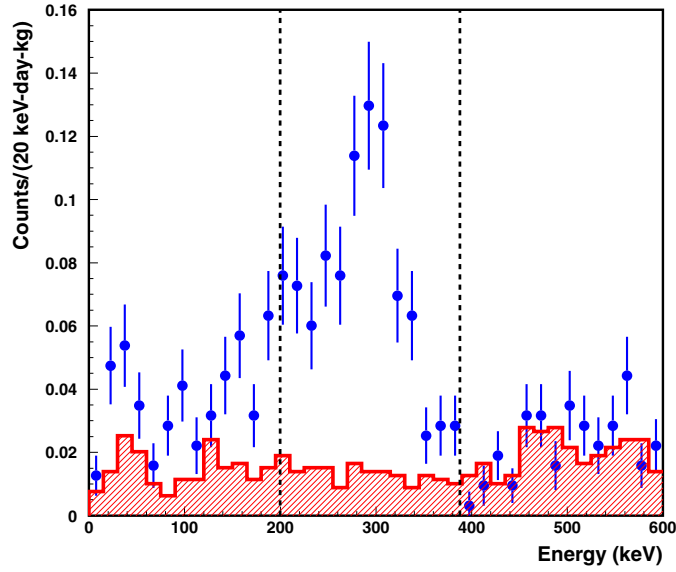
Figure 8. The Φ_{NaI}^- (blue data points) and Φ_{NaI}^+ (red histogram) spectra taken with the NaI(Tl) ACV detector. The photopeak at 300 keV can be tagged by the specified cuts, giving rise to the spectra of figure 7(b).

will be due to interactions of the surviving cosmic rays as well as to the fast neutrons produced by (α, n) reactions through natural ambient radioactivity.

4. Studies of possible neutrino-induced interactions

Neutrino interactions on nuclei were studied in counter experiments only for a few light isotopes (^{1}H [14], ^{2}H [15, 16] and ^{12}C [17]). For heavy nuclei, these were observed in radiochemical experiments (^{37}Cl [18] and ^{71}Ga [19]) but without timing and spectral information. Detailed theoretical work was confined mostly to these isotopes. Establishing more experimentally accessible detection channels will be of importance in the studies of nuclear structure and neutrino physics. For instance, interactions with lower threshold or better resolution than the $\bar{\nu}_e$-p inverse β^- decay and ν-d disintegration processes will open up new windows of investigations.

With reactor $\bar{\nu}_e$ as probes, neutrino-induced ^{73}Ge$^*(1/2^-)$ productions would manifest themselves as an excess of events for the reactor ON spectra [Φ_{Ge}^-(ON)] over that of the reactor OFF [Φ_{Ge}^-(OFF)]. Studies were performed on the tagged ^{73}Ge$^*(1/2^-)$ events discussed in previous sections.

4.1. Neutral-current nuclear excitation

Neutrino-induced neutral current processes have been observed in the disintegration of the deuteron with reactor $\bar{\nu}_e$ [15] and in the SNO experiment for solar ν_e [16]. For heavier isotopes, the interaction proceeds through neutral current excitation (NCEX) on nuclei via inelastic scattering

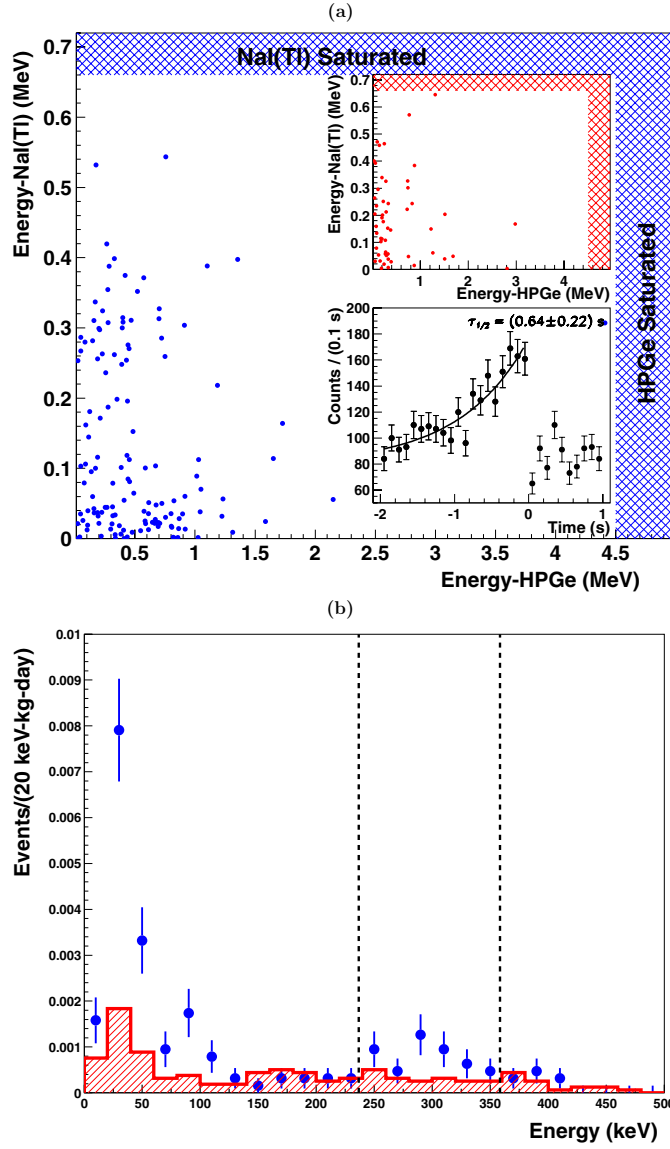$$\bar{\nu}_e + (A, Z) \rightarrow \bar{\nu}_e + (A, Z)^*. \tag{4}$$

9

Figure 9. (a) Scatter plots Φ_{NaI}^{-} versus Φ_{Ge}^{-} (blue) and Φ_{NaI}^{+} versus Φ_{Ge}^{+} (red in the inset) for events with cosmic-ray tag. Only events without saturating the electronics are shown, while the saturated ones are represented by the two bands. The timing distribution of the Φ_{Ge}^{-} events is displayed in the inset. (b) The corresponding Φ_{NaI}^{-} (blue data points) and Φ_{NaI}^{+} (red histogram) spectra are for the non-saturated events. The peak at 300 keV is an evidence of the cosmic-ray-induced production of ^{73}Ge* excited states.

This process was observed only in the case of ^{12}C [17] using accelerator neutrinos at energy of the order of O(10 MeV). Excitations at lower energies using reactor neutrinos have been studied theoretically [20, 21] but were not experimentally observed. This has been proposed as a detection channel for solar neutrinos for the isotope ^{11}B [22] and Dark Matter–WIMPs [23]. The NCEX processes are sensitive to the axial isoscalar component of the weak neutral currents and the strange quark content of the nucleon [24].

Table 2. Summary of the neutrino-induced NCEX and νCC studies, showing 90% CL limits on event rates and average cross sections.

NCEX channel	Δ (MeV)	E_γ (MeV)	Transitions	f_ν^Δ	ϵ_{Ge}	$\mathcal{R}_\nu^{NC}$ (kg^{-1} day^{-1})	$\langle\sigma_\nu^{NC}\rangle$ (cm^2)
^{73}Ge*(3/2$^-$)	0.364	0.297	$9/2^+ \to 3/2^-$	0.82	0.49	$<2.00 \times 10^{-2}$	$<1.13 \times 10^{-43}$
^{73}Ge*(3/2$^-$)	0.392	0.325	$9/2^+ \to 3/2^-$	0.80	0.45	$<4.36 \times 10^{-2}$	$<2.72 \times 10^{-43}$
^{73}Ge*(1/2$^+$)	0.555	0.488	$9/2^+ \to 1/2^+$	0.72	0.19	$<2.21 \times 10^{-2}$	$<3.24 \times 10^{-43}$
^{73}Ge*(1/2$^-$)	1.132	1.065	$9/2^+ \to 1/2^-$	0.45	0.15	$<3.12 \times 10^{-2}$	$<5.96 \times 10^{-43}$

νCC channel	Q (MeV)		Transition	f_ν^{Thr}	ϵ_{Ge}	$\mathcal{R}_\nu^{CC}$ (kg^{-1} day^{-1})	$\langle\sigma_\nu^{CC}\rangle$ (cm^2)
^{73}Ga(3/2$^-$)	1.665		$9/2^+ \to 3/2^-$	0.13	0.68	< 0.43	$<1.78 \times 10^{-42}$

The average cross section of the NCEX interactions in a neutrino beam with the spectrum $\phi_\nu(E_\nu)$ is given by, using the conventions of equation (6) of [20],

$$\langle\sigma_\nu^{NC}\rangle = \frac{\int_\Delta^\infty \sigma_\nu^{NC}(E_\nu)\phi_\nu(E_\nu)\,dE_\nu}{\Phi_\nu^{Total}}, \tag{5}$$

where Δ is the nuclear excitation energy and

$$\Phi_\nu^{Total} = \int_0^\infty \phi_\nu(E_\nu)\,dE_\nu \tag{6}$$

is the total neutrino flux. The energy dependence of the interaction cross section varies as [20]

$$\sigma_\nu^{NC}(E_\nu) \propto (E_\nu - \Delta)^2, \tag{7}$$

where the proportional constant depends on the weak couplings and nuclear matrix elements. The observed event rate is accordingly

$$\mathcal{R}_\nu^{NC} = \langle\sigma_\nu^{NC}\rangle \cdot \Phi_\nu^{Total} \cdot N_{Ge} \cdot \epsilon_{Ge}, \tag{8}$$

where N_{Ge} is the number of ^{73}Ge nuclei and ϵ_{Ge} is the detection efficiency, which can be evaluated by simulations.

The experimental signatures of NCEX for $(A, Z) = {}^{73}$Ge are the presence of mono-energetic lines at specified energies in the reactor $[\Phi_{Ge}^-(ON) - \Phi_{Ge}^-(OFF)]$ residual spectra. The candidate ^{73}Ge-NCEX channels and their respective ϵ_{Ge} are listed in table 2. Also shown is the fraction of the reactor neutrino flux above the kinematics threshold, given by

$$f_\nu^\Delta = \frac{\int_\Delta^\infty \phi_\nu(E_\nu)\,dE_\nu}{\Phi_\nu^{Total}}. \tag{9}$$

The residual spectra of the candidate transitions are depicted in figures 10(a)–(d). No excess of events were observed. Limits on $\mathcal{R}_\nu^{NC}$, and consequently on $\langle\sigma_\nu^{NC}\rangle$ at 90% CL, were derived and tabulated in table 2. The limiting sensitivities on $\langle\sigma_\nu^{NC}\rangle$ are typically factors of $\sim10^2$ worse than the typical range of $\sim10^{-45}$cm^2 predicted for the various isotopes [20, 21]. The dominant backgrounds are those of figure 7(a), where all the energy of the $\beta-\gamma$ emissions following ^{73}Ga decays were deposited in the HPGe.

4.2. Charged-current inverse beta decays

The neutrino-induced inverse β-decay reaction on the proton was the process on which the first observation of neutrinos was based [14]. Subsequently, there were several generations
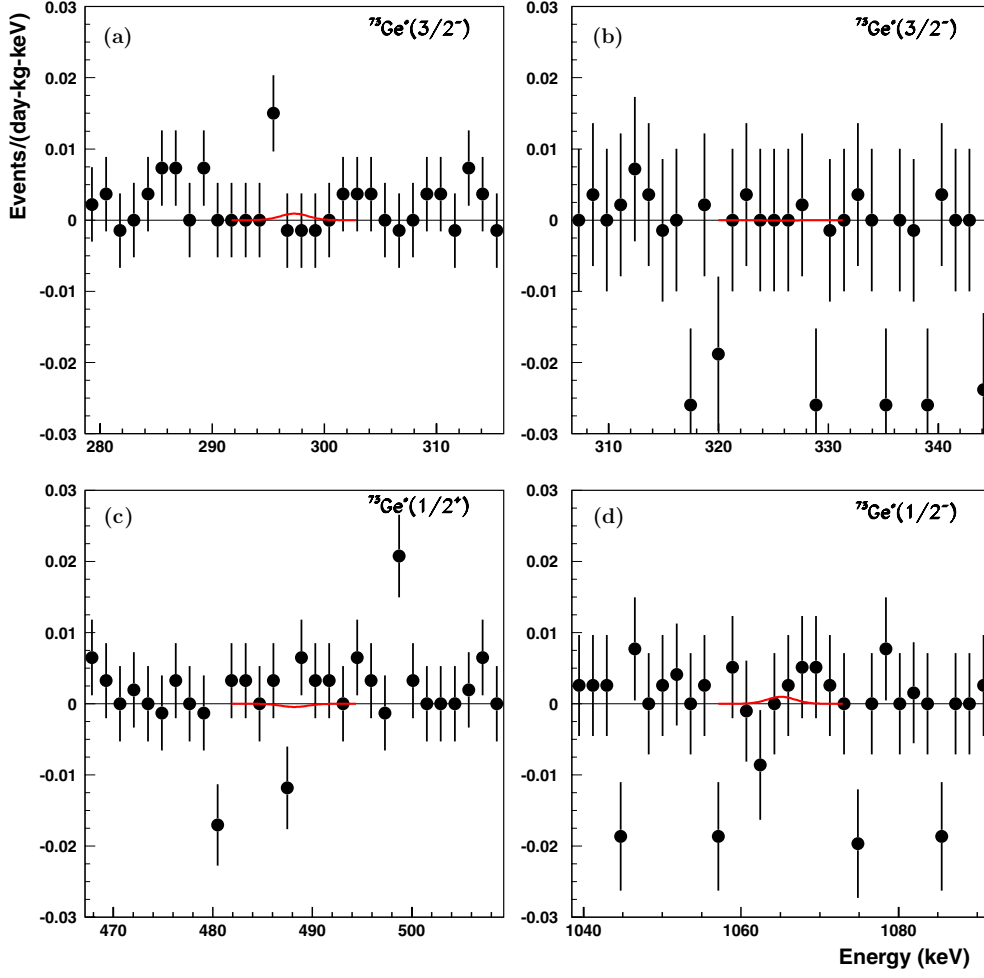
Figure 10. The $[\Phi_{Ge}^-(ON) - \Phi_{Ge}^-(OFF)]$ residual spectra for the four candidate channels for neutral-current excitation with the P3 data. The Gaussian best-fits are superimposed.

of oscillation experiments with reactor neutrinos that relied on this interaction. In addition, neutrino-induced charged-current processes were observed through the disintegration of the deuteron with reactor $\bar{\nu}_e$ [15] and in the SNO experiment for solar ν_e [16]. For heavy nuclei, charged-current interactions were observed only in solar ν_e through radiochemical experiments on ^{35}Cl [18] and ^{71}Ga [19]. There are still no successful real-time counter experiments yet, though there are intensive R&D efforts towards this goal [25]. The charged-current (νCC) inverse β-decay interaction for $\bar{\nu}_e$ on heavy nuclei such as ^{73}Ge is given by

$$\bar{\nu}_e + {}^{73}\text{Ge} \rightarrow e^+ + {}^{73}\text{Ga}^*. \tag{10}$$

Cases for other heavy isotopes were discussed in connection to the detection of low-energy $\bar{\nu}_e$ from the earth [26]. However, there are no experimental studies so far for these processes.

Signatures of νCC in ^{73}Ge manifest themselves as an excess of ^{73}Ga decay events for the reactor ON over OFF periods. The νCC rate $\left(\mathcal{R}_\nu^{CC}\right)$ is related to the average cross section via

$$\mathcal{R}_\nu^{CC} = \left\langle \sigma_\nu^{CC} \right\rangle \cdot \Phi_\nu^{Total} \cdot N_{Ge} \cdot \epsilon_{Ge}. \tag{11}$$

The interaction cross section varies with the neutrino energy as [26]

$$\sigma_\nu^{\mathrm{CC}}(E_\nu) \propto F(Z, E_+) \cdot E_+ \cdot \sqrt{E_+^2 - m_e^2}, \tag{12}$$

where $E_+ = E_\nu - Q - m_e$ is the positron energy and $F(Z, E_+)$ is the known nuclear Coulomb correction factor, and $Q = 1.67\,\mathrm{MeV}$ is the Q-value for the νCC interaction of equation (10).

As listed in table 2, the residual ^{73}Ga decay rate for the combined P1 and P3 periods is $R_\nu^{\mathrm{CC}} = (-0.94 \pm 0.67)\,\mathrm{day}^{-1}\,\mathrm{kg}^{-1}$, from which the 90% CL limits on R_ν^{CC} and $\langle\sigma_\nu^{\mathrm{CC}}\rangle$ were derived. The fractional $\bar{\nu}_e$-flux $\left(f_\nu^{\mathrm{Thr}}\right)$ follows the same definition as equation (9), with the threshold given by $\mathrm{Thr} = Q + m_e$. Similar to the case for NCEX, the sensitivities are limited by the cosmic-ray-induced ^{73}Ga and can therefore be enhanced in an underground location. There are no calculations on νCC rates with reactor neutrinos on heavy nuclei. Extrapolations from theoretical estimates on geo-neutrinos [26] suggest a general cross-section range of $\sim 10^{-44}\mathrm{cm}^2$ and hence factors of $\sim 10^2$ more stringent than the experimental bounds.

5. Summary and prospects

We made a thorough study on the decay signatures of the ^{73}Ge$^*(1/2^-)$ metastable state in a well-shielded reactor laboratory at a shallow depth of about 30 mwe. An unambiguous event-by-event tag of such decays was demonstrated, and studies of the signals within 2 s before the tag provide information on their production channels.

Searches for possible neutrino-induced nuclear transitions give rise to sensitivity limits which are typically factors of $\sim 10^2$ worse than the general predicted range. The background channels are all cosmic-ray induced, the most relevant one being the decays of ^{73}Ga. Consequently, the sensitivities can be greatly enhanced in an underground location. Physics experiments have been conducted in the past at the underground laboratory at the Krasnoyarsk reactor [27], though this facility is no longer available. Additional boost in the capabilities can be provided by position-sensitive segmented HPGe which can distinguish single-site from multi-site events.

Ton-scale isotopically-pure Ge-based detectors have been proposed and considered in the forthcoming double-beta decay experiments [5] in the case of ^{76}Ge, as well as cold dark-matter searches [7] where ^{73}Ge is ideal for studying the spin-dependent interactions. Background control and suppression are crucial to the success of these projects. Sophisticated procedures have been developed in the course of the R&D work. The unique three-fold timing correlations of the ^{73}Ge$^*(1/2^-)$ system demonstrated in this note will further enhance the background rejection capabilities.

A one-ton isotopically-pure ^{73}Ge detector located 15 m from a 3 GW reactor core would record ~ 16 neutrino-induced NCEX events per day at the typical predicted cross-section range of $10^{-45}\,\mathrm{cm}^2$ [20, 21]. The neutron flux in an underground site can be attenuated by a typical factor of 10^3 or more [28]. Therefore, a similar suppression in the ^{73}Ga background can be expected. The background levels of $<0.01\,\mathrm{kg}^{-1}\,\mathrm{day}^{-1}$ from table 2 for natural HPGe at surface would therefore imply a range of $<0.1\,\mathrm{ton}^{-1}\,\mathrm{day}^{-1}$ for pure ^{73}Ge detector underground. The detection of NCEX would be realistic and possible if an underground power reactor would be available.

Measurement of the low-energy solar neutrinos at a threshold low enough (<423 keV) to include the pp branch with the NCEX processes has important complementarity to the on-going efforts towards the detection of the charged-current interactions [25]. Using simple scaling between reactor and solar neutrino fluxes and spectra, the typical predicted cross-section ranges of [20, 21] correspond to a solar-ν-induced NCEX rate of $\sim 16\,\mathrm{ton}^{-1}\,\mathrm{year}^{-1}$ in a ^{73}Ge detector. This is comparable to the expected background range in an underground

location. Further optimizations on background control and suppression would make such a process observable.

Acknowledgments

References

[1] See *Review of Particle Physics*, Kayser B 2006 *J. Phys. G: Nucl. Part. Phys.* **33** 156 for details and references
[2] Wong H T 2004 *Mod. Phys. Lett.* A **19** 1207
[3] Wong H T and Li H B 2005 *Mod. Phys. Lett.* A **20** 1103
[4] See *Review of Particle Physics*, Vogel P and Piepke A 2006 *J. Phys. G: Nucl. Part. Phys.* **33** 479 for details and references
[5] Majorana Project 2006 *AIP Conf. Proc.* **842** 840
    GERDA Project 2006 *AIP Conf. Proc.* **842** 843
[6] See *Review of Particle Physics*, Drees M and Gerbier G 2006 *J. Phys. G: Nucl. Part. Phys.* **33** 233 for details and references
[7] Edelweiss Experiment 2006 *Phys. At. Nucl.* **69** 1967
    CDMS Experiment 2007 *AIP Conf. Proc.* **903** 579
[8] Li H B *et al* 2003 *Phys. Rev. Lett.* **90** 131802
    Wong H T *et al* 2007 *Phys. Rev.* D **75** 012001
[9] Xin B *et al* 2005 *Phys. Rev.* D **72** 012006
[10] Chang H M *et al* 2007 *Phys. Rev.* D **75** 052004
[11] Firestone R B *et al* 1996 *Table of Isotopes* 8th edn (New York: Wiley)
    Singh B 2004 *Nucl. Data Sheets* **101** 216
[12] Lai W P *et al* 2001 *Nucl. Instrum. Methods* A **465** 550
[13] Zhu Y F *et al* 2006 *Nucl. Instrum. Methods* A **557** 490
[14] Reines F and Cowan C L 1953 *Phys. Rev.* **92** 830
[15] Jenkins T L, Kinard F E and Reines F 1969 *Phys. Rev.* **185** 1599
    Pasierb E *et al* 1979 *Phys. Rev. Lett.* **43** 96
    Vidyakin G S *et al* 1988 *J. Exp. Theor. Phys.* **49** 151
    Vidyakin G S *et al* 1990 *J. Exp. Theor. Phys.* **51** 279
    Riley S P *et al* 1999 *Phys. Rev.* C **59** 1780
[16] Ahmad Q R *et al* 2002 *Phys. Rev. Lett.* **89** 011301
[17] Armbruster B *et al* 1998 *Phys. Lett.* B **423** 15
[18] Cleveland B T *et al* 1998 *Astrophys. J.* **496** 505
[19] Hampel W *et al* 1999 *Phys. Lett.* B **447** 127
    Abdurashitov J N *et al* 2002 *J. Exp. Theor. Phys.* **95** 181
[20] Lee H C 1978 *Nucl. Phys.* A **294** 473
[21] Donnelly T W and Reccei R D 1979 *Phys. Rep.* **50** 1
[22] Raghavan R S, Pakvasa S and Brown B A 1986 *Phys. Rev. Lett.* **57** 1801
[23] Goodman M W and Witten E 1985 *Phys. Rev.* D **31** 3059
    Ellis J, Flores R A and Lewin J D 1988 *Phys. Lett.* B **212** 375
[24] Bernabéu J *et al* 1992 *Nucl. Phys.* B **378** 131
    Kubodera K and Nozawa S 1994 *Int. J. Mod. Phys.* E **3** 101
    Kaplan D B and Manohar A 1988 *Nucl. Phys.* B **310** 527
    Garvey G *et al Phys. Rev.* C **48** 1919
[25] Raghavan R S 1976 *Phys. Rev. Lett.* **37** 259
    Raghavan R S 1997 *Phys. Rev. Lett.* **78** 3618
[26] Krauss L M, Glashow S L and Schramm D N 1984 *Nature* **310** 191
[27] Kozlov Yu V *et al* 2000 *Nucl. Phys.* B **87** 514
[28] Mei D M and Hime A 2006 *Phys. Rev.* D **73** 053004